University of Massachusetts Medical School

eScholarship@UMMS

2008-10-02

Sorting of EGF and transferrin at the plasma membrane and by cargo-specific signaling to EEA1-enriched endosomes

Deborah Leonard
University of Massachusetts Medical School

Et al.

Let us know how access to this document benefits you.

Follow this and additional works at: https://escholarship.umassmed.edu/oapubs

Part of the Life Sciences Commons, and the Medicine and Health Sciences Commons

Repository Citation

Sorting of EGF and transferrin at the plasma membrane and by cargo-specific signaling to EEA1-enriched endosomes

Deborah Leonard[1], Akira Hayakawa[1], Deirdre Lawe[1], David Lambright[1], Karl D. Bellve[2], Clive Standley[2], Lawrence M. Lifshitz[2], Kevin E. Fogarty[2] and Silvia Corvera[1,*]

[1]Program in Molecular Medicine and [2]Biomedical Imaging Group, University of Massachusetts Medical School, Worcester, Massachusetts 01605, USA

*Author for correspondence (e-mail: silvia.corvera@umassmed.edu)

Summary

The biological function of receptors is determined by their appropriate trafficking through the endosomal pathway. Following internalization, the transferrin (Tf) receptor quantitatively recycles to the plasma membrane, whereas the epidermal growth factor (EGF) receptor undergoes degradation. To determine how Tf and EGF engage these two different pathways we imaged their binding and early endocytic pathway in live cells using total internal reflection fluorescence microscopy (TIRF-M). We find that EGF and Tf bind to distinct plasma membrane regions and are incorporated into different endocytic vesicles. After internalization, both EGF-enriched and Tf-enriched vesicles interact with endosomes containing early endosome antigen 1 (EEA1). EGF is incorporated and retained in these endosomes, while Tf-containing vesicles rapidly dissociate and move to a juxtanuclear compartment. Endocytic vesicles carrying EGF recruit more Rab5 GTPase than those carrying Tf, which, by strengthening their association with EEA1-enriched endosomes, may provide a mechanism for the observed cargo-specific sorting. These results reveal pre-endocytic sorting of Tf and EGF, a specialized role for EEA1-enriched endosomes in EGF trafficking, and a potential mechanism for cargo-specified sorting of endocytic vesicles by these endosomes.

Introduction

EGF plays an important role in epithelial cell proliferation (Schlessinger et al., 1983; Yarden, 2001; Yarden and Schlessinger, 1985), and enhanced signaling through its receptor (EGFR) is implicated in the genesis of cancers of the lung, breast and brain. The major mechanism that limits EGF signaling is the rapid internalization and degradation of the activated EGFR, making the EGF-EGFR endocytic pathway an important locus for regulation of cell proliferation. In contrast to the EGFR, the transferrin (Tf) receptor (TfR), which, through binding di-ferric Tf is the major mechanism for delivery of iron into the cell, internalizes constitutively and is quantitatively recycled back to the plasma membrane following internalization. The molecular mechanisms that determine the marked differences in the itinerary of the endocytosed EGFR and the TfR are likely to play an important role in cellular growth and proliferation, and their disruption could underlie pathological alterations in these processes. However, when, where and by what mechanism these receptors are sorted from each other and into the different pathways of degradation and recycling is not entirely clear. One proposal is that EGFR and TfR internalize through a common pathway, and segregate after fusion with a common endosome in a dynein-regulated manner (Driskell et al., 2007). By contrast, it has also been proposed that these receptors are sorted after internalization into two distinct pre-endosome vesicle populations, which are then targeted to distinct populations of early endosomes with different maturation kinetics (Lakadamyali et al., 2006).

The origin and nature of the vesicular populations that carry EGFR or TfR with regard to their relative content of regulators of endosome dynamics, such as the small GTPase Rab5 or PtdIns(3)P-binding proteins is unclear. For example, Rab5 has been shown to be activated upon EGF binding and to be required for EGFR degradation (Barbieri et al., 2004; Barbieri et al., 2000), and Tf has been shown to transit through Rab5-enriched endosomes (Sonnichsen et al., 2000; Trischler et al., 1999). With regard to PtdIns(3)P binding proteins, EGFR degradation requires the ESCRT complex (Bache et al., 2003; Bache et al., 2006; Raiborg et al., 2001a; Raiborg et al., 2001b) which is localized to endosomes that contain PtdIns(3)P, but endosomal sorting complex required for transport (ESCRT) does not appear to influence TfR trafficking (Progida et al., 2007). However, another PtdIns(3)P-binding protein, the early endosome antigen-1 (EEA1), has been proposed to mediate early endosome fusion, as well as the capture of vesicles derived from clathrin-coated pits by early endosomes (Dumas et al., 2001; Merithew et al., 2003; Mills et al., 1998; Patki et al., 1997; Simonsen et al., 1998; Stenmark et al., 1996), and thus would be predicted to participate in trafficking of all types of cargo. All these results point to the involvement of Rab5 and PtdIns(3)P in both EGF-EGFR and Tf-TfR trafficking. However, the absence of a systematic analysis of trafficking of Tf and EGF relative to each

other, to Rab5, and to PtdIns(3)*P*-binding proteins such as EEA1 has impaired the generation of a testable, integrated model of the mechanisms of sorting of these ligands.

Here we have used total internal reflection fluorescence (TIRF) microscopy, an imaging technique in which fluorophores residing within approximately 100-300 nm from the plasma membrane can be selectively excited (Axelrod, 2001; Axelrod, 2003). We have coupled a TIRF microscope to a custom designed, highly sensitive CCD camera, with which we have recorded the trafficking of fluorescent EGF and Tf added simultaneously to cells for relatively long (30 minutes) periods of time with high temporal (0.5 frame/second) and spatial (160 nm/pixel) resolution. We have also analyzed the internalization of EGF and Tf in relation to Rab5 and EEA1. We observe that EGF and Tf segregate immediately upon binding to distinct plasma membrane domains, and can be seen in substantially distinct vesicle populations within 1 minutes after addition to the cell. Rapidly after internalization, vesicles containing EGF or Tf interact with EEA1-enriched endosomes. EGF-containing vesicles remain associated with and fuse with EEA1-enriched endosomes, while Tf-containing vesicles are released and move toward an EEA1-free, juxtanuclear recycling compartment. EGF-containing vesicles have a significantly higher concentration of Rab5 than Tf-containing vesicles, explaining their prolonged association and fusion with EEA1-enriched endosomes. Together these results suggest that the sorting of Tf and EGF is initiated at the plasma membrane and reinforced during endocytosis, through the selection by EEA1-enriched endosomes of incoming endocytic vesicles containing cargo destined for degradation.

Results

Visualization of the early steps of EGF and Tf trafficking

The initial steps of fluorescent ligand binding and internalization can be visualized in real time using TIRF, because of the receptor-mediated concentration of ligand at the cell surface. Thus, we used this methodology to compare the binding and trafficking of fluorescent Tf and EGF in cells maintained under constant physiological temperature and buffer conditions. Both ligands were added simultaneously to COS-7 cells, which contain endogenous receptors for both ligands, and were removed by three rapid washes with 35°C buffer, 2 minutes after addition. Imaging began just before the addition of ligands, with the incident angle of the laser set to image ~100 nm from the coverslip. Following the wash, the incident angle was changed to image deeper into the cell, ~300 nm from the coverslip (Fig. 1; Movie 1 in supplementary material). EGF and Tf bound to the cell surface within 60 seconds after addition, but in very different patterns: the Tf signal comprised both diffuse and concentrated patches distributed over the entire adherent surface, which we and others have previously shown to be regions of clathrin enrichment (Bellve et al., 2006; Merrifield et al., 2005). By contrast, EGF was mostly seen in smaller spots that tended to concentrate around the periphery of the cell. There was very little overlap between the EGF and Tf signals at these early time points. Despite the largely non-overlapping initial distribution, significant colocalization between Tf and EGF could be seen between 3 and 6 minutes (Fig. 1, 180-360 seconds) after addition of the ligands, in vesicular structures generally located between the edge of the cell and the juxtanuclear region. Within this same time period, Tf accumulated in a tight juxtanuclear region (Fig. 1, 60-600 seconds), while EGF remained in more peripheral vesicular structures. These increased in size as they decreased in number, and very gradually moved to the perinuclear region after 10-15 minutes of EGF binding,

remaining separate from the Tf-enriched recycling endosome (Fig. 1, 600-1500 seconds). Thus colocalization between EGF and Tf is restricted to a narrow window of time.

To rule out the possibility that these observations could be due to chromatic aberration, or to differences attributable to the dyes used to label the ligands, we compared the images obtained when cells were exposed to mixtures of Alexa-Fluor-488- and Alexa-Fluor-568-conjugated Tf, Alexa-Fluor-488- and Alexa-Fluor-568-conjugated EGF, or Tf and EGF coupled to different fluorophores. We then analyzed images obtained 5 minutes after addition of the ligands, when the maximal colocalization between Tf and EGF was observed. As expected, when the same ligand conjugated to two different fluorophores was added, the signals observed were largely overlapping (Fig. 2A, top and middle rows), whereas mostly non-overlapping signals were observed when cells were incubated with EGF and Tf each coupled to a different fluorophore (Fig. 2A, bottom row). At higher temporal resolution, it is evident that when the same ligand, coupled to a different fluorophore is used, both signals move in a correlated manner, whereas when two different ligands are analyzed the movement is not correlated (Fig. 2B, arrows). To obtain a quantitative measure of the degree of overlap, masked, binary images of the two fluorophores were generated from the raw data as described previously and in Materials and Methods (Bellve et al., 2006). This method is highly stringent, as the degree of colocalization will decrease substantially as a function of relatively small differences in fluorophore brightness, differences in cellular autofluorescence in the red or green channels, and expected chromatic aberrations due to focus and wavelength variation. Thus, the average colocalization between fluorophores was of ~60% (percentage of green colocalized with red, and percentage of red colocalized with green) when the same ligand was labeled with different fluorophores, and did not vary over time (Fig. 2C). The maximal colocalization observed when EGF and Tf coupled to different fluorophores were added was seen at ~360 seconds after addition, and was significantly lower (see below).

To quantify the colocalization between EGF and Tf over time, both the total number of pixels over background for each fluorophore, and the number of colocalized pixels was plotted over time (Fig. 3). Non-specific (spurious) colocalization was calculated using image segments rotated 180°, as described previously. Specific signal over background for the two fluorophores was detected almost immediately after addition of ligands (Fig. 3A,B). At these early time points (0-90 seconds) very few pixels colocalized, less than 10% of either signal (Fig. 3C). Within 3-6 minutes however, significant colocalization between EGF and Tf was observed (Fig. 3D), amounting to 20-30% of the pixels visualized (Fig. 3G). The number of EGF pixels in the TIRF zone remained fairly constant between 6-20 minutes, whereas the number of Tf pixels decreased continuously (Fig. 3F), as a result of the movement to the juxtanuclear region, or out of the cell through fast recycling. The disappearance of Tf signal paralleled the loss of colocalized pixels. To rule out the possibility that the signals visualized at the earliest time points corresponded to plasma membrane domains, as opposed to early endocytic vesicles, we analyzed the effects of acid washing on a cell exposed to EGF and Tf for 90 seconds (Fig. 3H). Both before and after acid washing Tf and EGF signals were distinct and there was only minor overlap. Together these results suggest strongly that EGF and Tf are segregated immediately upon binding and that this segregation is maintained during internalization, distributing the ligands into different vesicles. Soon thereafter, both types of vesicles appear to interact either with each other or with
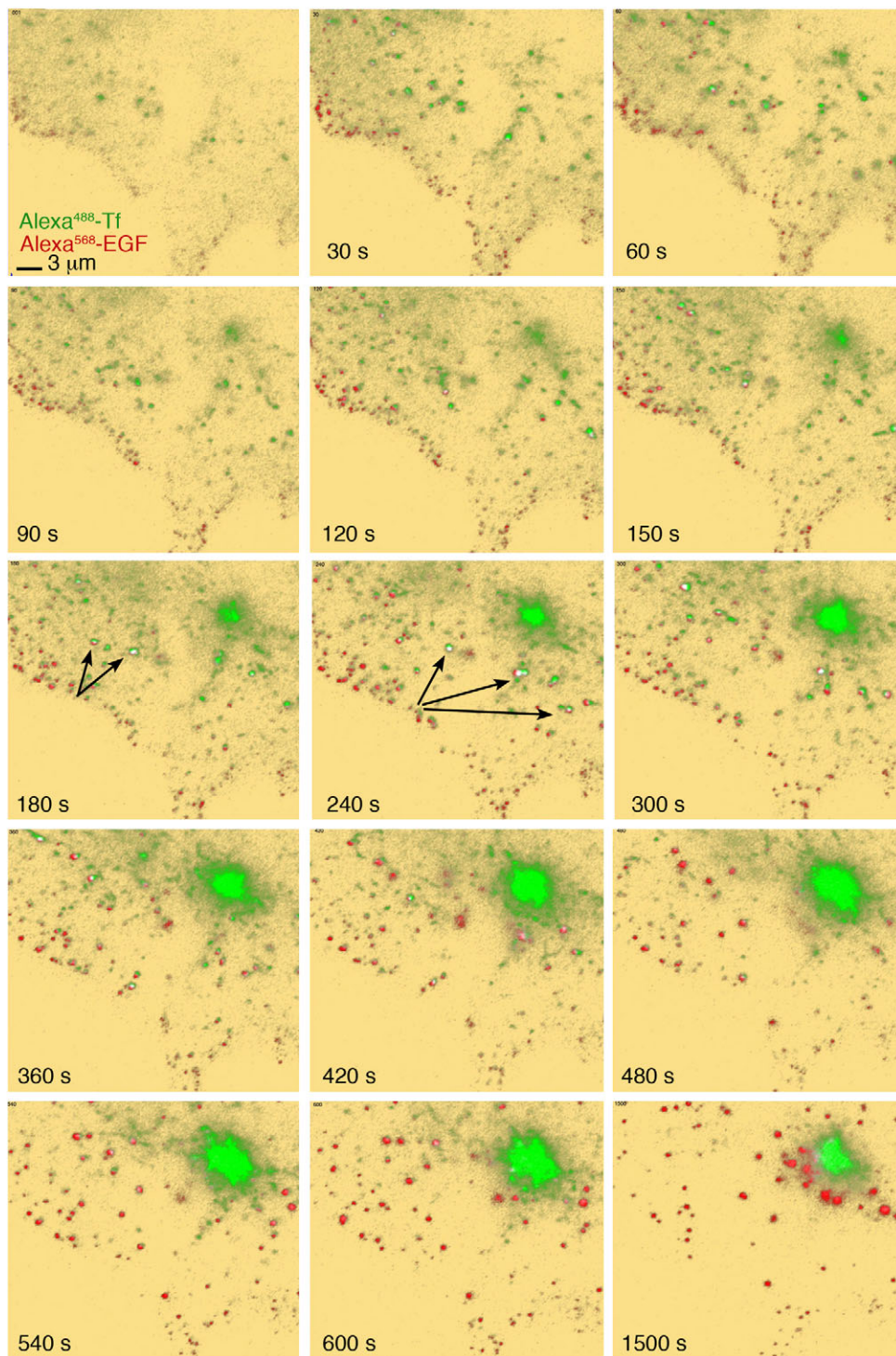
Fig. 1. Binding and internalization of EGF and Tf in COS-7 cells. COS-7 cells grown on coverslips were placed in KRH buffer at 35°C, and exposed to 50 ng/ml Alexa-Fluor-568–EGF and 20 µg/ml Alexa-Fluor-488–Tf. Image capture was started immediately after ligand addition. Background is pseudo colored in yellow to enhance low level signal. Colocalized signal (arrows) is pseudo colored in white. The complete time series can be seen in Movie 1 in supplementary material.

a common structure within 300 nm from the plasma membrane, such that the fluorescent ligands cannot be optically resolved, and significant colocalization is measurable. Subsequently, EGF persists in this structure, while Tf moves to the juxtanuclear region and/or rapidly recycles out of the cell.

The segregation of EGF and Tf immediately upon binding could be due to either different distributions of their respective receptors within the plasma membrane, or differences in the affinity of such receptors for their ligand as a function of their plasma membrane

localization. To better understand the basis for the differences in binding between EGF and TF, we analyzed the localization of their receptors (Fig. 4). Cells were exposed to un-labeled EGF and Tf for different periods of time, fixed, permeabilized and stained with antibodies to the EGFR and TfR (Fig. 4A). Optical sections through the cell were acquired and projected into a single two-dimensional (2D) image. In addition, images were deconvoluted (Patki et al., 2001) to remove out of focus blur and allow imaging in the z-axis to distinguish dorsal and ventral plasma membrane regions (Fig.

4B). These results indicate that the TfR is homogeneously distributed on the dorsal and ventral plasma membrane regions, and is predominantly intracellular in the presence or absence of ligand. The EGFR also appears homogeneously distributed on the dorsal and ventral aspects of the plasma membrane, but clearly concentrates along the peripheral edges of the cell (arrows) and in a juxtanuclear region probably corresponding to elements of the secretory pathway. Upon addition of EGF, the EGFR disappears from the plasma membrane and is predominantly found in endocytic structures. The distribution and response of the receptor matches closely that seen in live cells when visualizing fluorescent EGF, and indeed,

colocalization of Alexa-Fluor-568–EGF with internalized EGFR was very extensive (Fig. 4C). Thus, the differences in EGF and Tf binding seen by TIRF is likely to be due to the differences in distribution of their respective receptors at steady state.

### Trafficking of Tf and EGF relative to EEA1
To determine the relationship between early endosomes containing EEA1 and early endocytic vesicles containing EGF or Tf, cells were transiently transfected with an EEA1-N-terminal GFP-tagged construct. EEA1-containing endosomes could be seen within 300 nm from the coverslips (Fig. 5A). No clear colocalization between
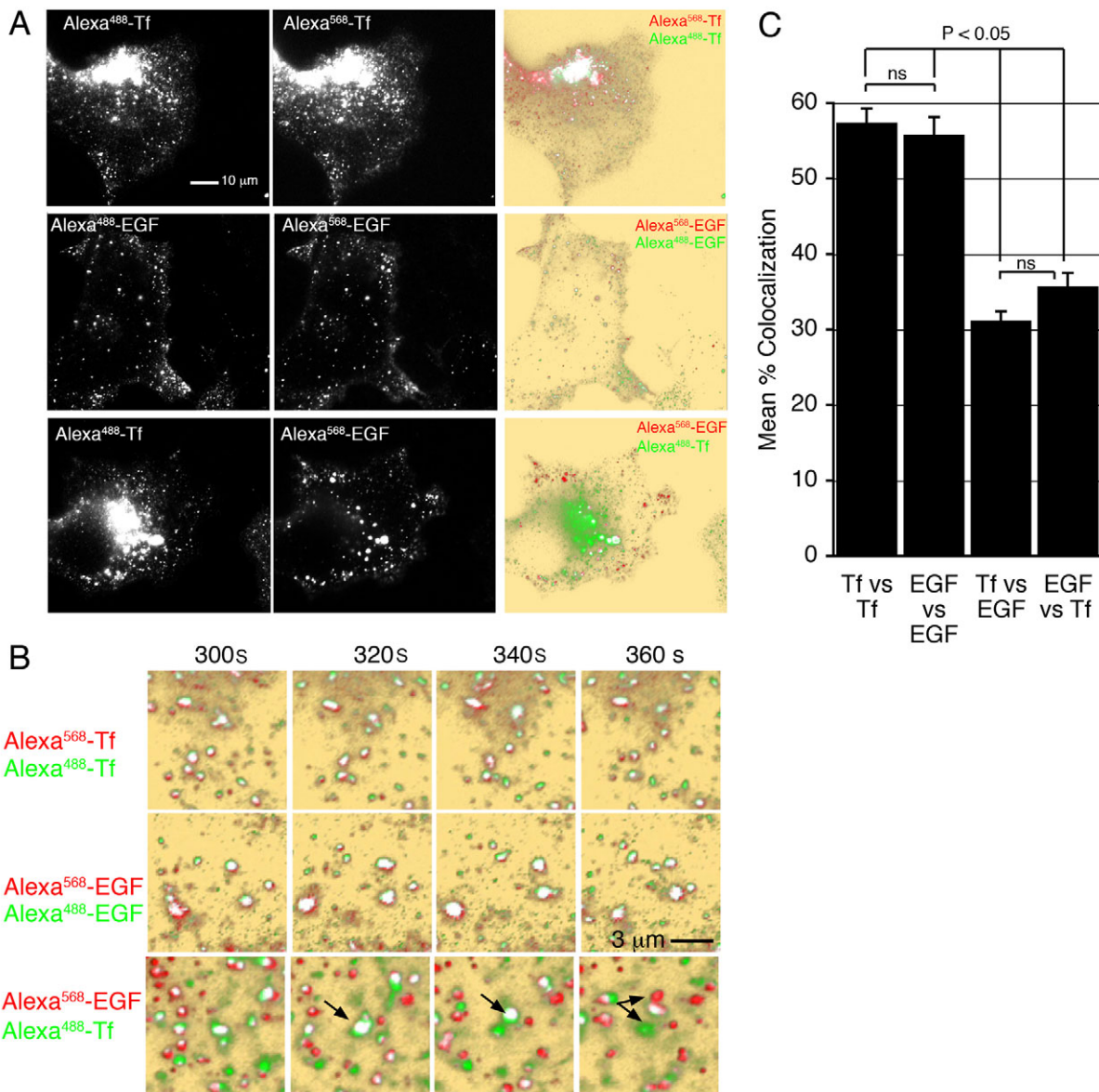

Fig. 2. Imaging of ligand pairs conjugated to different fluorophores. (A) COS-7 cells grown on coverslips were placed in KRH buffer at 35°C, and exposed to 10 μg/ml Alexa-Fluor-488–Tf + 10 μg/ml Alexa-Fluor-568–Tf (top panels), 50 ng/ml Alexa-Fluor-568–EGF + 50 ng/ml Alexa-Fluor–488-EGF (middle panels), or 50 ng/ml Alexa-Fluor-568–EGF + 10 μg/ml Alexa-Fluor-488–Tf (bottom panels) for 5 minutes. (Right panels) Merged images showing the overlap. (B) Images from the time periods after addition of ligands indicated above the panels. Arrows indicate the clear segregation of signals seen in cells incubated with different ligands, that is not seen with the same ligand conjugated to two different fluorophores. (C) Quantification of signal overlap between fluorophores after 5 minutes of exposure. Values are mean ± s.e.m. of five different experiments. Statistical significance of the differences between groups was estimated using two-tailed Student's *t*-tests.

Tf and EEA1 was observed in the first 2 minutes after addition of ligand (not illustrated). Subsequently, colocalization could be seen, albeit most of the colocalized pixels were in regions of high pixel density where individual vesicular structures were not readily discernible over the more diffuse Tf background. Observation of individual endosomes indicates that Tf-containing vesicles come into close proximity to EEA1-enriched endosomes, but this localization is transient, and Tf does not remain associated for long

with the EEA1 signal (Fig. 5A,B, arrows). To determine whether Tf interacts more stably with EEA1-enriched endosomes that may be outside the TIRF zone, cells were exposed to Tf for 2 minutes, washed in the presence of unlabeled Tf, and imaged by TIRF-M, alternating with epifluorescence to acquire optical sections through the entire volume of the cell at 60 second intervals. The TIRF-M image preceding the switch to epifluorescence, and the projection of the optical sections into single 2D images is shown in Fig. 5C.
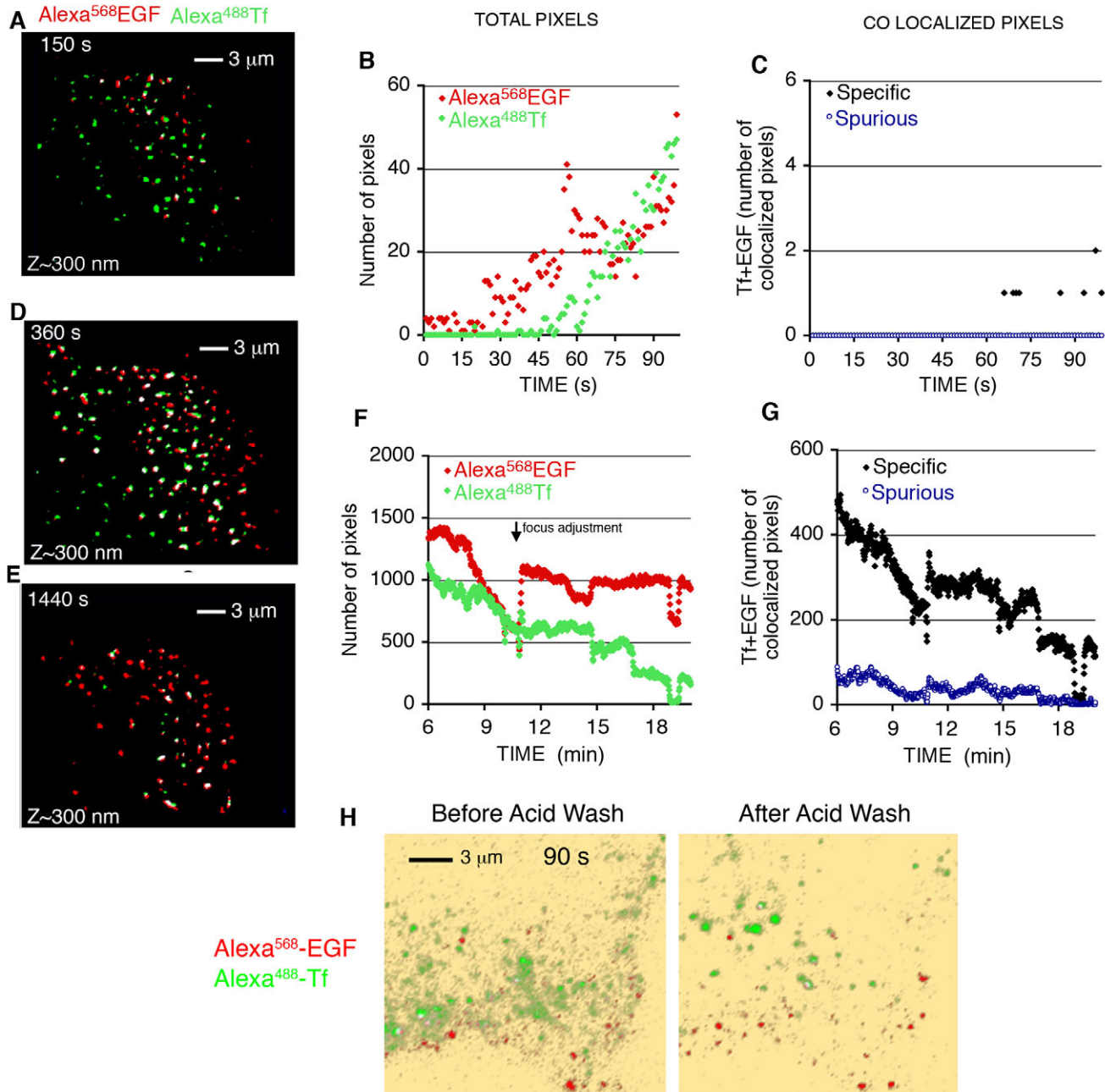
Fig. 3. Quantification of the dynamics of EGF and Tf binding, internalization and colocalization. COS-7 cells grown on coverslips were placed in KRH buffer at 35°C, and exposed to 50 ng/ml Alexa-Fluor-568–EGF and 20 µg/ml Alexa-Fluor-488–Tf. Image capture was started immediately after ligand addition, with the incident angle of the laser set to visualize ~100 nm from the coverslip. After 2 minutes, cells were washed twice with KRH and the incident angle modified to visualize ~300 nm into the cell. Masked, overlapped images from several time points are shown in A,D and E. The number of total pixels of each fluorophore (B,F), as well as the number of colocalized pixels (C,G) seen at early time points after ligand addition (B,C), and after the wash step (F,G) are plotted over time after ligand addition. Results are from a single image set which is representative of a minimum of five independent experiments. (H) Cells were exposed to ligands for 90 seconds, imaged, washed in cold PBS, exposed to an acid wash solution for 3 minutes, and re-imaged.
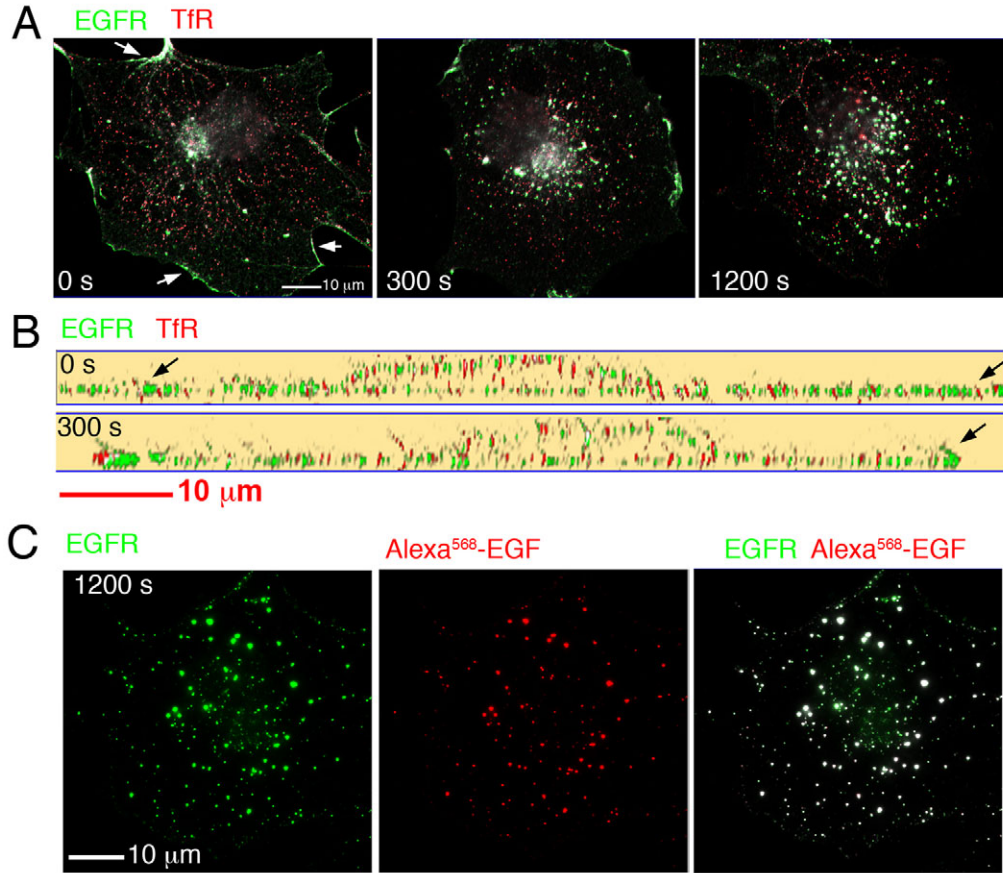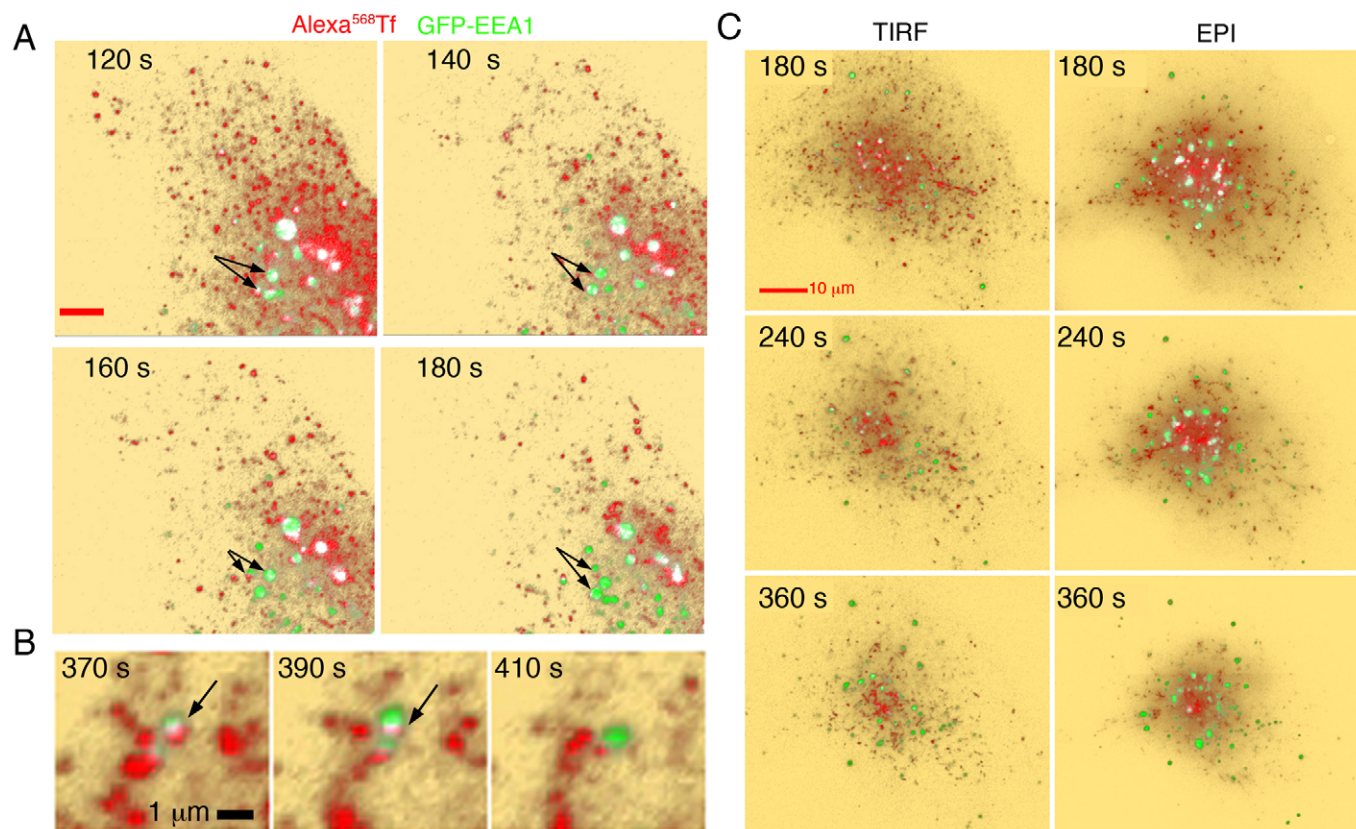
Fig. 4. (A) COS-7 cells were exposed to unlabeled EGF and Tf for the times indicated, fixed and stained with antibodies to the EGFR and the TFR. Optical sections were obtained at 250 nm intervals through the entire volume of the cell, and projected into a single 2D image. A clear demarcation of the cell edge was seen with antibodies to EGFR (arrows), but not to the TfR. (B) 130 nm optical slices through the thickest part of the nuclei of cells treated and stained as in A (arrows indicate localization of EGFR). (C) Cells were exposed to Alexa-Fluor-568–EGF for 20 minutes, fixed, and stained with antibodies to the EGFR. Optical sections were obtained at 250 nm intervals through the entire volume of the cell, and projected into a single 2D image.

In both TIRF-M and epifluorescence images, partial colocalization between Tf and EEA1 is seen between 2-3 minutes following ligand addition, but, within 6-8 minutes the majority of Tf is localized to a juxtanuclear region largely devoid of EEA1-enriched endosomes (Fig. 5C). Thus, it appears from these images that many, but perhaps not all, Tf-containing vesicles might dock with EEA1-enriched endosomes, but may detach without fusing and progress to the perinuclear region. A few vesicles may actually fuse, and Tf then be more slowly sorted out. The stochastic variation in the ability of Tf-containing vesicles to fuse with EEA1-enriched endosomes may explain the existence of different pools of Tf that recycle at different rates (Maxfield and McGraw, 2004)

The trafficking of EGF relative to EEA1 was very different than that of Tf. Colocalization between EGF and EEA1 was seen after 4-5 minutes of addition of ligand, even in areas of low EEA1 and EGF signal density (Fig. 6A, white pixels, arrowheads). After 5-6 minutes, the majority of EEA1-enriched endosomes contained EGF. Observation of individual endosomes at higher resolution (Fig. 6B, arrows) indicated that vesicles containing EGF become enriched in EEA1, come into close proximity of larger EEA1-enriched endosomes, and appear to fuse. In addition, in approximately 30% of cells, large ring-like EEA1-containing endosomes appeared at the periphery of the cell (Fig. 6A, arrows). Vesicles containing EGF became attached to these ring structures, resulting in significant colocalization between the two fluorophores. The appearance of these endosomes was not observed in the absence of EGF, and could be quantified as a small but statistically significant increase in the mean intensity of EEA1 signal in the TIRF zone (748±14 versus 914±5 arbitrary fluorescent intensity units; mean ± standard

deviation before and after the addition of EGF; n=3, P<0.05). To determine whether the interactions between EGF and EEA1 seen in the TIRF zone reflect the trafficking of the ligand in regions of the cell invisible by TIRF-M, we acquired optical sections through the entire volume of the cell after EGF addition. Cells were exposed to EGF for 2 minutes, washed, and optical sections obtained at 60-second intervals and projected into single 2D images (Fig. 6C). As seen by TIRF-M, EGF entered the cell in small vesicular structures that interacted with EEA1-labeled endosomes within 5 minutes after addition. The formation of ring-like EEA1-enriched structures in response to EGF was also readily observed. Thus, the trafficking of EGF visualized in the TIRF zone reflects the trafficking of the receptor outside this region.

The quantitative analysis of the interactions between EGF and EEA1 and Tf and EEA1 are shown in Fig. 7. The percentage of EEA1 pixels that colocalized with EGF was much greater (50-60% of EEA1 pixels colocalized with EGF), and persisted over time (Fig. 7A), than the colocalization of EEA1 with Tf, which was much lower (<20%, after subtraction of spurious colocalization values), and decreased rapidly over time (Fig. 7B) as Tf moved to the juxtanuclear region (Fig. 7C). Because these differences in colocalization might only reflect differences in receptor trafficking kinetics giving rise to differing density of ligand, we also analyzed the percentage of each ligand colocalized with EEA1 in regions where both fluorophores were present (i.e. excluding the juxtanuclear compartment where a large amount of Tf concentrates and very few EEA1-enriched endosomes are observed) at different time points after ligand addition. Although after 4-5 minutes of incubation the percentage of total ligand colocalized with EEA1

Fig. 5. Imaging of Tf and EEA1. (A) COS-7 cells expressing GFP-EEA1 (green) were exposed to 10 μg/ml Alexa-Fluor-568–Tf (red) for the times indicated in each panel. After 60 seconds cells were washed, incubated with 200 μg/ml unlabeled Tf, and imaged by TIRF-M with an incident angle set to visualize 300 nm from the coverslip. Colocalized voxels are depicted in white. (B) Higher resolution series depicting the transient nature of the colocalization of Tf with EEA1. (C) TIRF images were obtained at 0.5 Hz, and at 60-second intervals illumination was switched to epifluorescence for the acquisition of optical sections at 250 nm intervals through the entire cell volume. Shown is the TIRF image preceding the acquisition of the image stack. Optical sections were projected into a single 2D image. Arrows in A and B indicate the movement of Tf-containing vesicles as they near EEA1-enriched endosomes; however, colocalization is brief because the Tf structures move away from the EEA1 signal.

was similar between EGF and Tf, the percentage of colocalized EGF increased with time, whereas that of Tf remained unchanged (Fig. 7D). Together these results indicate that EGF and Tf enter through distinct classes of endocytic vesicles, which have different post-endocytic behaviors. EGF-enriched vesicles rapidly associate and EGF remains associated with EEA1-enriched endosomes, whereas Tf-enriched endocytic vesicles move rapidly to the juxtanuclear recycling endosome with no significant dwell time in EEA1-enriched endosomes. The significant overlap between the EEA1 and EGF signals suggest that EGF-containing vesicles fuse with EEA1-enriched endosomes, whereas Tf-enriched vesicles can not.

Role of EEA1

The results shown above indicate that EEA1-enriched endosomes play a different role in the trafficking of EGF compared with Tf, but the specific role of EEA1 itself is not clear. Both in-vitro and in-vivo data suggest that EEA1 serves as a tether that facilitates endosome fusion through its interactions with Rab5. According to this model, depletion of EEA1 would result in generalized defects in endosomal trafficking. However, the results shown above suggest a more specialized role for EEA1 in EGFR trafficking. To test this hypothesis, we studied the effects of EEA1 depletion using RNA interference in COS-7 cells. However, within 24 hours of

transfection with siRNA oligonucleotides directed to EEA1, cells ceased to divide, and by 48 hours had lifted off the plate (not illustrated). This response was seen with numerous different specific oligonucleotides to EEA1, but not with scrambled oligonucleotides. To address this problem, we generated a stable HeLa cell line harboring lower amounts of EEA1. A HeLa cell line was selected (KD cells), in which the levels of EEA1 mRNA were <30% of those in controls (Fig. 8A). The levels of EEA1 protein were decreased by 80-90% as assessed by western blot analysis and immunofluorescence (Fig. 8B). The rate of EGF-stimulated EGFR degradation was slower in the KD cells than in the control cells (Fig. 8C). By contrast, the rates of Tf uptake and recycling were similar between control and KD cells (Fig. 8D). These results are consistent with the finding that EEA1-enriched endosomes play a selective role in EGFR trafficking, and suggest that EEA1 itself is important in this process. Moreover, they reveal an unexpected important role for EEA1 in cell survival, which will require further study.

### Trafficking of Tf and EGF relative to Rab5

The results shown above indicate that vesicles containing EGF interact strongly with endosomes enriched in EEA1, whereas Tf-containing vesicles interact more weakly. One of the important early regulatory factors that influences the interaction among endocytic
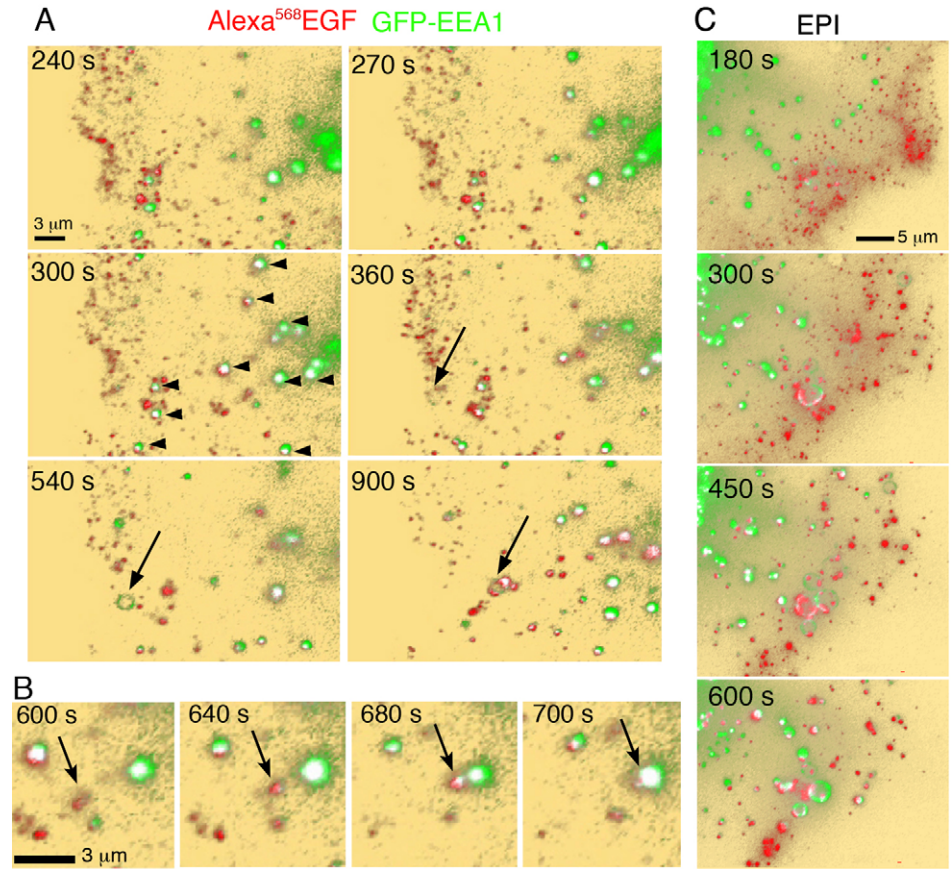
Fig. 6. Imaging of EGF and EEA1.
(A) COS-7 cells expressing GFP-EEA1 (green) were exposed to 50 ng/ml Alexa-Fluor-568–EGF (red) and imaged for the times after ligand addition, as indicated in each panel. After 3 minutes cells were washed and imaged by TIRF-M with an incident angle set to visualize 300 nm from the coverslip. Colocalized voxels are depicted in white, and indicated with arrowheads. Arrows point to the appearance of a ring-like structure containing EEA1, to which EGF-containing vesicles appear to attach. (B) Higher resolution series depicting the association of EGF-containing vesicles (arrow) with EEA1-enriched endosomes. (C) Optical sections at 250 nm intervals through the entire cell volume were projected into a single 2D image.
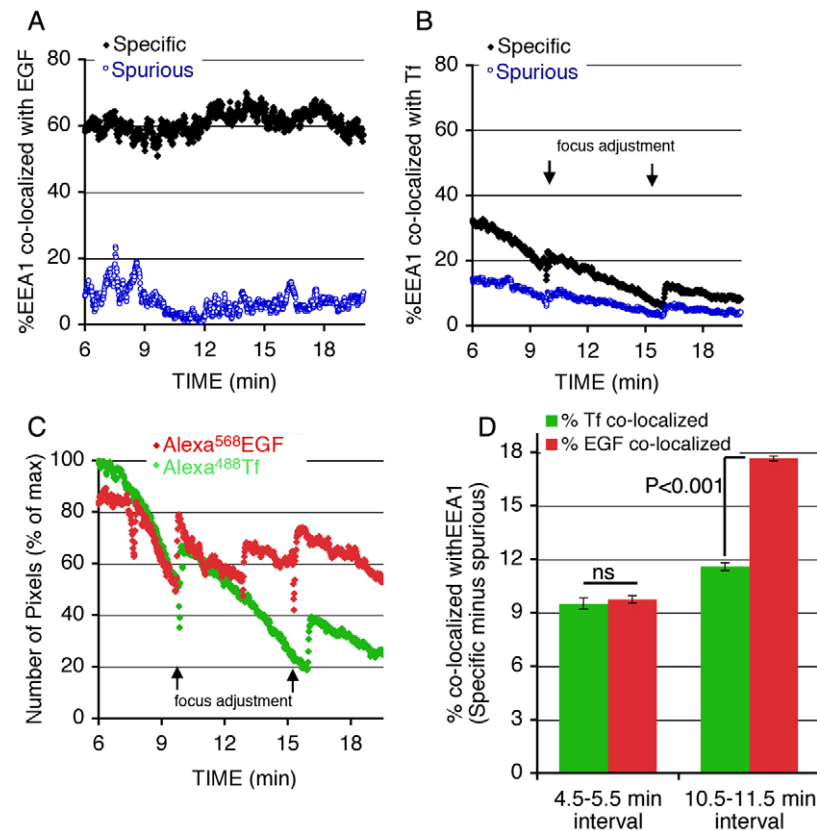
Fig. 7. Quantification of EGF and Tf colocalization with EEA1. COS-7 cells expressing GFP-EEA1 were exposed to 50 ng/ml Alexa-Fluor-568–EGF (A,C) or 10 μg/ml Alexa-Fluor-568–Tf (B,C) for 5 minutes, after which fluorophores were washed and unlabeled Tf added at a concentration of 200 μg/ml (B,C). Plotted are the percentage of total EEA1 pixels colocalized with EGF (A) or Tf (B) over time. (C) Number of total pixels of each fluorophore over time, normalized to the maximum seen immediately after the wash step. (D) Percentage of Tf or EGF pixels colocalized with EEA1 in regions containing both fluorophores at indicated times after exposure to ligands. Results are from a single image set which is representative of a minimum of five independent experiments.

vesicles and endosomes is the GTPase Rab5. EEA1 is known to interact with Rab5, via specific recognition domains in its C and N termini (Lawe et al., 2002; Merithew et al., 2003; Simonsen et al., 1998). Thus, differences in Rab5 content or activation might underlie the propensity of vesicles to fuse with EEA1-enriched endosomes. To explore whether Rab5 content of endocytic vesicles containing Tf or EGF might differ, cells transiently transfected with GFP-Rab5 were analyzed. To control for variations in the level of expression of Rab5 that could influence trafficking dynamics of either ligand, we used the same cell to consecutively analyze the trafficking of Tf and EGF relative to GFP-Rab5.

Epifluorescence imaging revealed the majority of Rab5 to be localized in the perinuclear region, with numerous smaller highly dynamic vesicular structures localized towards the cell periphery. This steady state localization did not change during exposure to Tf (Fig. 9A, left panels), but, in response to subsequent addition EGF, structures containing Rab5 increased in abundance at the cell periphery (Fig. 9A, right panels). Quantification of this effect revealed that it was due to a redistribution of Rab5 from the juxtanuclear region, which occurred within 5 minutes after exposure of cells to EGF (Fig. 9B). TIRF-M images of ligand internalization into these cells revealed very different dynamics between the interaction of Tf-containing vesicles and EGF-containing vesicles with Rab5 (Fig. 9C). Colocalization between Tf and Rab5 was seen very early after ligand addition, but was transient. By contrast, colocalization between Rab5 and EGF was seen in many more vesicles containing EGF, and increased with time. These images also reveal that the redistribution of Rab5 from the juxtanuclear region to the cell periphery coincided with its colocalization with EGF-containing endocytic vesicles (Fig. 9C, right panels, arrows), resulting in a quantitative difference in the proportion of total Rab5 signal colocalizing with EGF compared with Tf (Fig. 9D). These results suggest that the concentration of Rab5 that associates with EGF-containing vesicles is higher than that which associates with Tf-containing endocytic vesicles. In addition, Rab5 activation occurs rapidly in response to EGF binding, possibly increasing the concentration of Rab5 in vesicles containing activated EGFR. This later possibility is supported by analysis of EGF internalization in Rab5-expressing cells at higher temporal resolution (Fig. 9E), where Rab5 appears to associate with very peripheral structures containing EGF within 2-3 minutes of ligand addition. This time course precedes the interaction of EGF-containing vesicles with EEA1-enriched endosomes shown above, consistent with the possibility that Rab5 activation in response to EGF might determine its targeting to EEA1-enriched endosomes.

Discussion

The process of ligand sorting in the endocytic pathway entails changes in the localization of relatively low abundance receptors and ligands within the three-dimensional volume of a single cell continuously over time. Thus, the ideal experimental approach to this multidimensional problem would include high detection sensitivity, high spatial resolution and high temporal resolution,
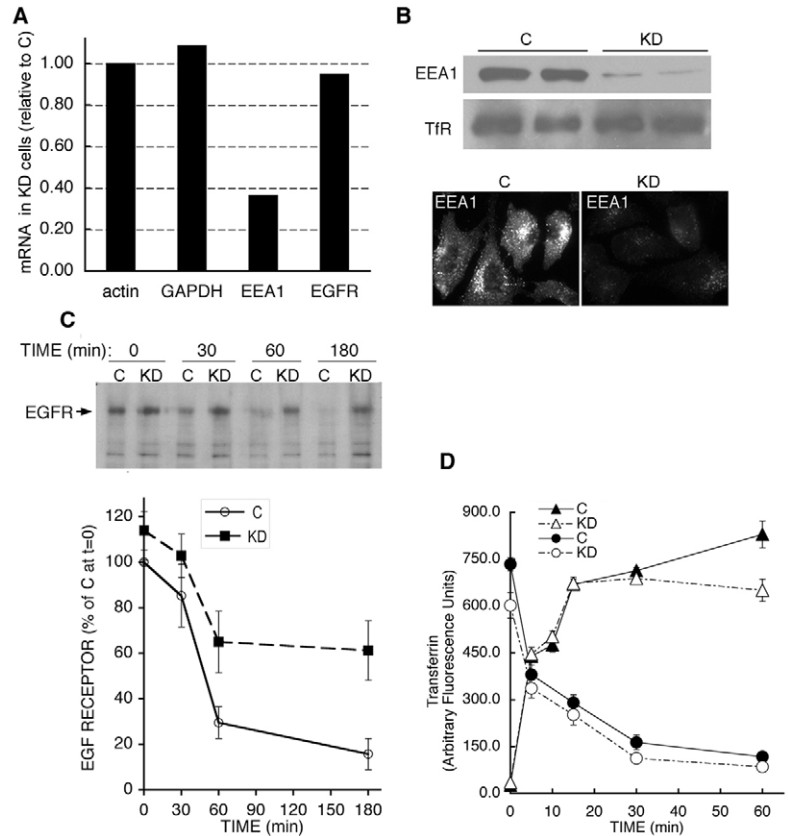
Fig. 8. Effect of EEA1 knockdown on Tf and EGF trafficking. (A) Real time quantitative PCR in HeLa cells stably expressing a scrambled control (C) or an EEA1-directed (KD) shRNA. The mRNAs examined are indicated along the *x*-axis. (B) Western blotting of EEA1 and TfR in two independent stable clones, and immunofluorescence analysis of EEA1. (C) Cells were serum starved and incubated in the presence of EGF for the times indicated. Extracts were analyzed by western blotting with anti-EGFR antibodies. Values are mean ± s.e.m. of four independent experiments analyzed by densitometric scanning. (D) Kinetics of Tf uptake and recycling in C and KD cells. Values are mean ± s.e.m. of three experiments performed in duplicate.

applicable to live cells grown under physiological conditions and exposed to physiological concentrations of ligands. The development of TIRF-M, highly sensitive CCD cameras and rapid acquisition hardware and software platforms approximates this ideal, by allowing the direct observation of low abundance fluorophores at high temporal resolution in live cells, with improved resolution stemming from the selective illumination of the region of the cell where endocytosis occurs. These new tools can be used to re-address important, long standing questions that have been addressed previously with existing methodologies. In this paper, we present images of the binding and internalization of fluorescent EGF and Tf, added simultaneously at physiological concentrations to cells that contain endogenous receptors for these ligands held at physiological temperature and buffer conditions. These results show that the plasma membrane regions containing the receptors to which these two ligands bind are distinct and segregated, and that ligand segregation largely persists throughout the endocytic process. Similar results were seen in HeLa and Hepa1-6 hepatoma cells (not shown). Thus, the initial sorting of EGF and Tf receptors into separate endocytic routes initiates with their distinct distribution at the plasma membrane, and persists during the endocytic route of these receptors. The itineraries of endocytic vesicles containing EGF
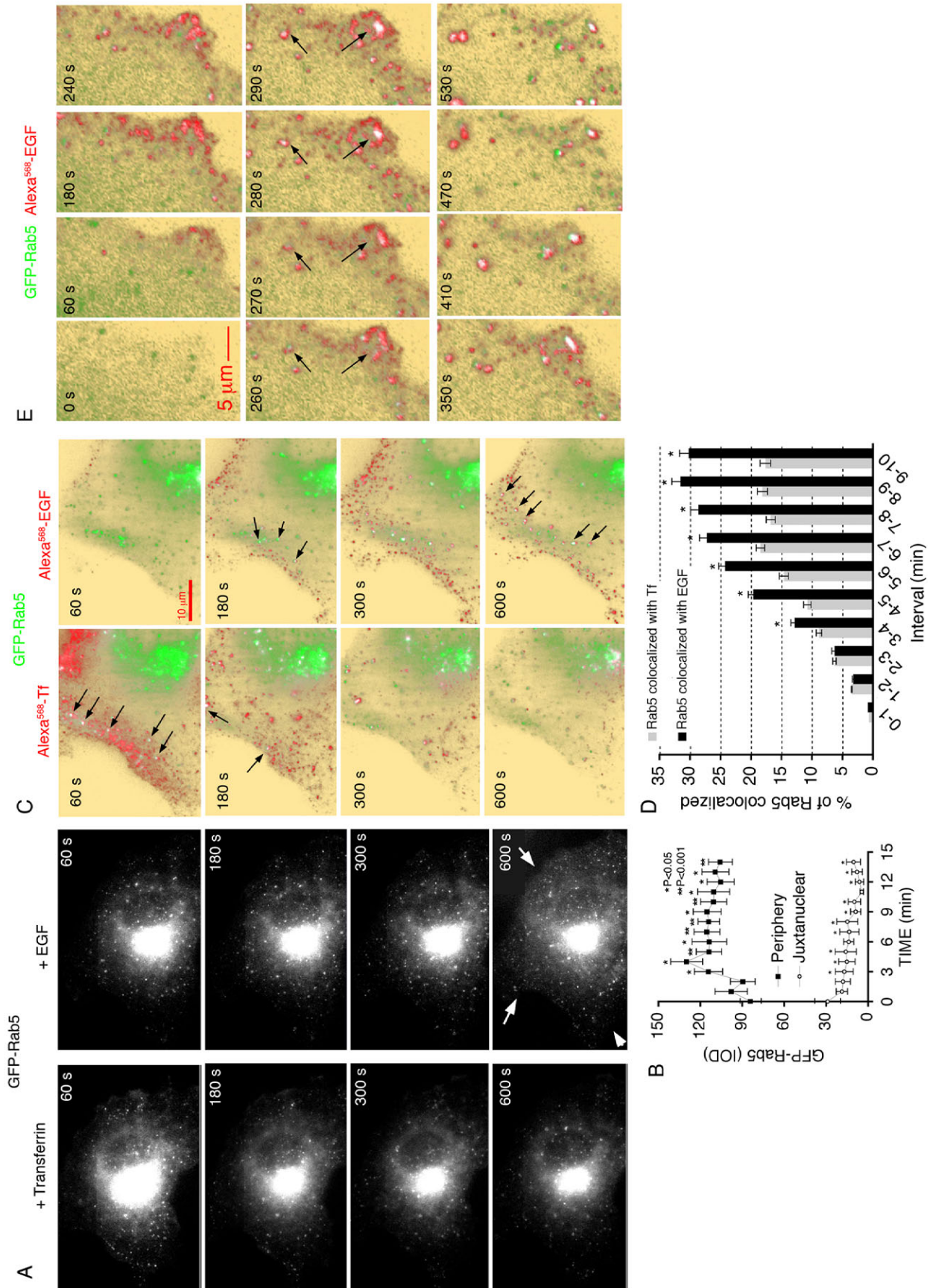
Fig. 9. See next page for legend.

or Tf intersect at a common point along the endocytic pathway, consisting of endosomes enriched in EEA1. EGF-containing vesicles commit to the EEA1 pathway, whereas Tf-containing vesicles do not. Thus, EEA1-enriched endosomes constitute a second sorting point where vesicles can be segregated based on their cargo.

The finding that EGF and Tf are internalized into different endocytic vesicles appears to be at odds with conventional understanding of the pathway of internalization of these ligands. Numerous prior studies have concluded that EGF and TF are internalized through clathrin-coated pits into similar endocytic vesicles, which fuse with a sorting endosome from which Tf-TfR complexes are removed to undergo recycling, and EGF-EGFR complexes undergo inward vesiculation and targeting to late endosomes and lysosomes. Many of the studies leading to this model were based on biochemical analysis of isolated endosomal membranes, sometimes combined with electron microscopy (Dickson et al., 1983; Hanover et al., 1984; Hopkins, 1985; Willingham et al., 1983; Willingham et al., 1984), and led to the important observation, consistent with our studies, that TfR internalize constitutively by clathrin-coated pits, whereas EGF receptors internalize only upon ligand binding through more complex endocytic mechanisms. However, these studies were largely hampered by low sensitivity, making it necessary to use cell lines expressing abnormally high receptor levels (e.g. A431 cells) and/or introduce manipulations to enhance ligand density, such as incubation of cells at low temperatures (4-20°C) for extended periods of time (60-90 minutes) with saturating ligand concentrations prior to analysis. These manipulations can potentially distort the normal dynamics of endocytosis. Nevertheless, careful analysis of the primary results of several of these important early contributions reveals that even under these conditions, the distribution of EGF and Tf during endocytosis in purified endosome subfractions was quite different at the earliest time points measured. Moreover, discrepancies in the kinetics of clearance of EGFR from the cell surface and their appearance in endosomes enriched with TfR led to speculation that vesicles containing newly internalized EGF and Tf receptors may arise as separate populations (Futter and Hopkins, 1989). Moreover, early studies involving short pulses with radiolabled EGF and Tf in fibroblasts reached the conclusion that the majority of cell-bound Tf was segregated from EGF (Gorman

and Poretz, 1987). Early studies using fluorescent tracers and video microscopy in live cells revealed complexities in the endocytic pathway not anticipated by electron microscopy studies or biochemical approaches, and revealed significant differences in the pathway of internalization of Tf and EGFR (Hopkins et al., 1990). Given the advantages of newer technologies, a re-visitation of the problem of Tf-TfR and EGF-EGFR endocytic sorting seemed warranted. The results presented here, using these technologies, suggest that EGF-EGFR and Tf-TfR follow distinct routes of internalization under physiological conditions. This hypothesis will ultimately have to be tested with the positive identification and characterization of the molecular components of these endocytic pathways.

The existence of different early endocytic carriers that vary in their motility and cargo content (Lakadamyali et al., 2006) has been pointed out recently. However, the mechanism by which ligand-receptor complexes reach these endocytic carriers is not clear. Our results, consistent with numerous prior studies, indicate substantial segregation of EGFR and TfR at the plasma membrane. This could lead to internalization from these regions directly into separate endocytic carriers, or to migration of receptors from their localization to common sites of entry, followed by rapid segregation into distinct endocytic vesicles (Tosoni et al., 2005). It is largely accepted that Tf-TfR complexes are pre-clustered and internalized by clathrin-coated membrane regions, and this process is very evident using the platform utilized in our current study, where extensive colocalization between Tf and clathrin is seen almost immediately after exposure of cells to Tf, followed by progression into endocytic vesicles devoid of clathrin (Bellve et al., 2006). Given the lack of colocalization of EGF with Tf at early time points of binding and throughout early internalization seen in this current study, we favor the possibility that internalization of the majority of EGF occurs through regions devoid of clathrin. This view is consistent with studies that find EGFR within lipid rafts (Mobius et al., 1999; Pike et al., 2005) and macropinosomes (Hamasaki et al., 2004; Orth et al., 2006), and recent studies using image correlation spectroscopy report that 90% of the EGFR is correlated with rafts in COS-7 cells, before and after ligand binding (Keating et al., 2007). These results are consistent with the existence of alternative internalization pathways for EGF (Sigismund et al., 2005; Yamazaki et al., 2002). Nevertheless, the distinct endocytic mechanisms used by EGF and Tf may share similar regulatory controls, including the requirement for dynamin and accessory proteins that have been shown to be necessary for both EGF and Tf receptor internalization (Puri et al., 2005; Sorkina et al., 2002). More work will be required to define the biochemical and functional features that make these pathways unique, beyond their common regulatory control mechanisms.

A surprising finding in this study was the very large difference in the extent of association of EGF and Tf with EEA1-enriched endosomes. The colocalization of EEA1 with Tf reported by ourselves and others (Lawe et al., 2002; Mills et al., 1998; Patki et al., 1997; Simonsen et al., 1998; Stenmark et al., 1996) has contributed to the notion that EEA1 may be involved in the internalization and sorting of Tf and other ligands by mediating early endosome fusion events. These colocalization studies have been relatively non-quantitative with respect to the percentage of total cellular associated Tf colocalizing with EEA1, and of the percentage of EEA1-enriched endosomes containing Tf over time, and have not systematically compared Tf with EGF. The new results shown here suggest a model where, rather than being a universal

Fig. 9. Imaging of GFP-Rab5c, Tf and EGF. (A-C) COS-7 cells expressing GFP-Rab5c were exposed to Alexa-Fluor-568–Tf for 3 minutes followed by a wash and addition of unlabeled Tf at a concentration of 200 µg/ml. Cells were imaged continuously by TIRF-M alternating with epifluorescence as described above. After 30 minutes, when the vast majority of the Tf signal had disappeared from the cell, Alexa-Fluor-568–EGF was added, and imaging resumed. (A) Optical sections through the cell in the GFP channel, illustrating the distribution of Rab5 in the three-dimensional volume of the cell. Arrows point to the redistribution of Rab5 to the cell periphery in response to EGF. (B) The mean intensity of Rab5 in the peripheral and juxtanuclear regions over time after exposure to EGF was quantified in five independent cells. (C) TIRF images of the fluorescent ligands superimposed on the Rab5 image. Arrows point to regions of colocalization. (D) Colocalization between Rab5-GFP and Alexa-Fluor-568–EGF or Alexa-Fluor-568–Tf over time. Plotted are the percentage of Rab5 colocalized with each ligand in pixel-dense regions (two to three regions per cell) over the indicated time intervals. Values are mean ± s.e.m. of three independent experiments. Statistical significance was calculated from two-tailed paired Student's *t*-tests. *$P<0.001$. (E) Sequence of images of a cell expressing GFP-Rab5 and exposed to Alexa-Fluor-568–EGF for the times shown in each panel. Arrows point to regions containing Alexa-Fluor-568–EGF, which acquire GFP-Rab5. Similar results were observed in a minimum of five independent experiments.
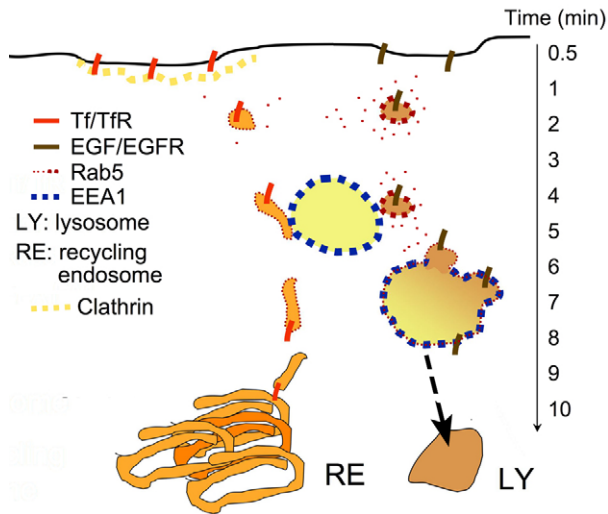
Fig. 10. Model for Tf and EGF internalization and sorting relative to EEA1. The majority of liganded EGFR and TfR internalize through distinct plasma membrane regions, entering into vesicles that contain Rab5. The active EGFR recruits more Rab5 resulting in a higher density of this GTPase in EGF-containing vesicles compared to Tf-containing vesicles. Both types of vesicles interact with EEA1-enriched endosomes, but only EGF-containing vesicles can interact strongly, and fuse. Tf-TfR-containing vesicles move to the perinuclear recycling endosome, while the EGF-EGFR complex is now sequestered by EEA1-enriched endosomes. In this model, EEA1 marks the entry point into the degradative pathway.

marker of early endocytic vesicles and endosomes, EEA1 specifically marks a point of entry into the degradative pathway (Fig. 10). This notion is consistent with studies describing the presence of EEA1 in subsets of endosomes that had already suggested a more specific function for this protein (Wilson et al., 2000). In this context, EEA1 may work in conjunction with the proteins Hrs and ESCRT to direct the degradation of EGFR (Bache et al., 2003; Katzmann et al., 2003). Moreover, EEA1-depleted cells display no changes in the kinetics of uptake or recycling of Tf, but show a delay in EGFR degradation, consistent with the central conclusion of our studies of a differential role of EEA1-enriched endosomes in EGF and Tf sorting. However, one important caveat is that acute depletion of EEA1 is unexpectedly lethal, and cells selected to withstand low levels of EEA1 may have compensated by mechanisms that could indirectly affect EGF receptor trafficking. Thus, more work is needed to define the basis for the role of EEA1 both in cell survival, and in the trafficking of vesicles enriched in EGF.

Among the possible features that distinguish early endocytic vesicles and that could account for the selective fusion of vesicles containing EGF with EEA1-enriched endosomes is the concentration of Rab5. This GTPase was found to be rapidly recruited to early endocytic vesicles containing EGF (Fig. 9E), a result consistent with the observed rapid activation of this GTPase by EGF (Barbieri et al., 2000), and its requirement for EGF receptor degradation. Furthermore, dominant interfering mutants of Rab5 impair EGFR degradation without impairing initial internalization (Dinneen and Ceresa, 2004). Importantly, the rapid acquisition of Rab5 by EGF-containing vesicles may be due to the direct binding of Rab5 exchange factors by the activated EGFR (Penengo et al., 2006; Su et al., 2007), resulting in cargo-specific recruitment and activation of Rab5 by specific vesicles. This can

lead to enhanced association of EGF-containing vesicles with EEA1-enriched endosomes, and thus provide a mechanism for selection of cargo destined to this specific pathway. By contrast, lower levels of Rab5 may be sufficient to mediate formation and internalization of Tf-containing vesicles, but insufficient for their retention by EEA1-enriched endosomes, allowing the movement of these vesicles away from these endosomes and into the recycling pathway. Further work will be required to determine the precise mechanisms of activation of Rab5 by EGF, and determine the role of these mechanisms in mediating the selective interaction of EGF-enriched vesicles with EEA1-enriched endosomes uncovered in this study.

Materials and Methods

Optical system
Epifluorescence imaging was done using a Zeiss Axiovert 200 inverted microscope with a Zeiss 100× 1.40 NA oil-immersion objective and equipped with a Zeiss AxioCam HR CCD camera with 1300×1030 pixel resolution. For TIRF imaging, two Coherent Innova 70C lasers are used. Argon ion and argon-krypton ion lasers were used to produce the 488 and 568 nm light, respectively. The combined beams were coupled into a single mode fiber using a KineFLEX fiber coupler manufactured by Point Source (Hamble, UK). A modified Olympus IX81 inverted microscope, a modified Olympus TIRF fiber illuminator and an Olympus Plan APO 60× objective with an NA of 1.45 were used. TIRF illumination was introduced through the edge of the objective at an angle set between 65° and 68° giving a penetration depth of 90-121 nm at 488 nm and 105-141 nm at 568 nm. Light is collimated through the objective and a layer of immersion oil onto the coverslip. The quality of the collimation was set halfway between the best for 488 nm and 568 nm. Light from the fluorophores was collected and relayed onto a 640×448 pixel CCD camera developed with Lincoln Labs (MIT). A Physik Instruments pifoc was used for fine focus control. The entire microscope was contained in a heated chamber held at 35°C. Imaging hardware and software were previously described (Bellve et al., 2006).

Image analysis
For quantitative image analysis, the following strategy was used. First, raw images were corrected by subtracting the background fluorescence outside the cell. Second, a running average of three time points with a total of interval of 4 seconds was generated, which removed slight speckling due to camera noise but had a negligible effect on the data. Third, to generate images in which structured fluorescence (i.e. vesicles) can be quantitatively analyzed without interference from background diffuse fluorescence, images were smoothed by convolving with a small, 2D Gaussian spot (s=160 nm) that preserved the mean intensity. The local background was estimated by convolving with a larger, 2D Gaussian (s=320 nm) and subtracting this from the smoothed images. From this a binary masking image was generated by setting the intensity of all positive-valued pixels to one and all other pixels to zero. This mask was multiplied by the original image to display areas in the image with intensity exceeding the average local background. Colocalized pixels were identified from the overlap of the masked images of each ligand. Spurious colocalization was defined as that seen when pixel-rich regions were rotated 180 degrees relative to each other.

Fluorescent probes, antibodies and cells
Alexa-Fluor-labeled probes were obtained from Molecular Probes (Invitrogen). Anti-EGFR antibodies were from Upstate. Anti-TfR antibodies were from BD-Transduction Labs. Rab5c and EEA1 constructs were generated as previously described (Lawe et al., 2002; Lawe et al., 2000). In the experiments described here, COS-7 cells were transfected using 1-4 μg of plasmid DNA using calcium phosphate (Invitrogen), and imaged 48 hours later. Cells were transferred from complete medium to KRH [125 mM NaCl, 5 mM KCl, 1.3 mM CaCl$_2$, 1.2 mM MgSO$_4$, 25 mM HEPES pH 7.4, 2 mM sodium pyruvate and 0.5% BSA (bovine serum albumin)] just prior to imaging. All imaging procedures were performed at 35°C.

qRT-PCR
Total RNA was extracted with Trizol® reagent. After RNase-free DNase I digestion, RNA was purified with Qiagen RNeasy® MinElute™ cleanup kit. The purified RNA was then used to synthesize cDNA (iScript™ cDNA Synthesis Kit). Real-time PCR was performed with iQ™ SYBR® Green Supermix on a MyiQ single-color real-time PCR detection system from Bio-Rad. The $2^{-\Delta\Delta C_T}$ method was used to analyze the relative mRNA level. Ferritin heavy chain mRNA was used as internal control.

Binding studies
Cells were seeded at 1×10^5 cells/well in 6-well plates in DMEM containing antibiotics and 10% FBS. Cells were serum-starved for 2 hours and incubated with Alexa-Fluor-594–Tf (20 mg/ml) at 37°C for the times indicated in each experiment. Cells were then placed on ice, washed twice with ice-cold PBS and incubated for 5 minutes in acidic

buffer (0.2 M acetic acid, 0.5 M NaCl in ddH$_2$O) to remove non-internalized ligand. Cells were washed twice in ice-cold PBS, harvested, centrifuged for 20 minutes at 1200 *g* at 4°C, resuspended in 100 μl ice-cold PBS and added to wells on a 96-well plate. For Tf recycling studies, cells were incubated with Alexa-Fluor-594–Tf (20 μg/ml) at 37°C for 2 hours, washed twice with ice-cold PBS, and then placed at 37°C for the times indicated before harvesting. The fluorescence intensity of each well was measured using a plate reader at excitation/emission wavelengths of 594/625 nm. Non-specific binding was calculated using 100-fold excess of non-fluorescent ligand. The protein concentration in each well was then measured using the BCA protein assay kit (Pierce), and the fluorescence value normalized to the amount of protein per well. Statistical analyses were done using two-tailed paired Student's *t*-tests.

EEA1 knockdown

An shRNA directed to EEA1 was cloned into a p*Silencer* 3.1-H1 puro (Ambion) as a 54-nucleotide hairpin loop, between restriction sites *Bam*HI and *Hind*III using the oligos: sense, 5′-GGATCCGAAGCCTGTTCGTGTCTGTTTCAAGAGAACAGA-CACGAACAGGCTTCTTTTTTGGAAA-3′, and antisense 5′-AGCTTTTCCA-AAAAAGAAGCCTGTTCGTGTCTGTTCTCTTGAAACAGACACGAACAGG-CTTCG-3′. Insert sequence was confirmed by DNA sequencing. The construct was then used for stable transfection in HeLa cells using FuGENE6 transfection reagent (Roche). HeLa cells were also transfected with a negative control vector (pSilencer-negative) provided by Ambion. The negative control vector has a shRNA insert the sequence of which is not found in the human or mouse database. Two days after the transfection, puromycin (Sigma-Aldrich) was used for selection.

EGFR degradation studies

Cells were plated at 1×10^5 cells per well of a 6-well tissue culture dish, and allowed to grow overnight in DMEM containing puromycin. The next day cells were serum-starved for 30 minutes before treatment with 50 μM cycloheximide (EMD Biosciences) for 60 minutes. Serum-free conditions and treatment with cycloheximide were continued through the duration of the experiment. Cells were then incubated with EGF (Molecular Probes) at 1 μg/ml for the time indicated. Cells were then placed on ice, washed twice with ice-cold PBS and lysed in 100 μl of PBS-TDS buffer (10 mM dibasic sodium phosphate, 150 mM sodium chloride, 1% Triton X-100, 0.5% sodium deoxycholate, 0.1% sodium dodecyl sulfate, 0.2% sodium azide, 0.004% sodium fluoride, pH 7.25) with protease inhibitors. Nuclei were removed and samples were analyzed by western blot using the Western Lighting system (PerkinElmer).

References

Axelrod, D. (2001). Total internal reflection fluorescence microscopy in cell biology. *Traffic* **2**, 764-774.

Axelrod, D. (2003). Total internal reflection fluorescence microscopy in cell biology. *Meth. Enzymol.* **361**, 1-33.

Bache, K. G., Brech, A., Mehlum, A. and Stenmark, H. (2003). Hrs regulates multivesicular body formation via ESCRT recruitment to endosomes. *J. Cell Biol.* **162**, 435-442.

Bache, K. G., Stuffers, S., Malerod, L., Slagsvold, T., Raiborg, C., Lechardeur, D., Walchli, S., Lukacs, G. L., Brech, A., Stenmark, H. et al. (2006). The ESCRT-III Subunit hVps24 is required for degradation but not silencing of the epidermal growth factor receptor. *Mol. Biol. Cell* **17**, 2513-2523.

Barbieri, M. A., Roberts, R. L., Gumusboga, A., Highfield, H., Alvarez-Dominguez, C., Wells, A. and Stahl, P. D. (2000). Epidermal growth factor and membrane trafficking. EGF receptor activation of endocytosis requires Rab5a. *J. Cell Biol.* **151**, 539-550.

Barbieri, M. A., Fernandez-Pol, S., Hunker, C., Horazdovsky, B. H. and Stahl, P. D. (2004). Role of rab5 in EGF receptor-mediated signal transduction. *Eur. J. Cell Biol.* **83**, 305-314.

Bellve, K. D., Leonard, D., Standley, C., Lifshitz, L. M., Tuft, R. A., Hayakawa, A., Corvera, S. and Fogarty, K. E. (2006). Plasma membrane domains specialized for clathrin-mediated endocytosis in primary cells. *J. Biol. Chem.* **281**, 16139-16146.

Dickson, R. B., Hanover, J. A., Willingham, M. C. and Pastan, I. (1983). Prelysosomal divergence of transferrin and epidermal growth factor during receptor-mediated endocytosis. *Biochemistry* **22**, 5667-5674.

Dinneen, J. L. and Ceresa, B. P. (2004). Expression of dominant negative rab5 in HeLa cells regulates endocytic trafficking distal from the plasma membrane. *Exp. Cell Res.* **294**, 509-522.

Driskell, O. J., Mironov, A., Allan, V. J. and Woodman, P. G. (2007). Dynein is required for receptor sorting and the morphogenesis of early endosomes. *Nat. Cell Biol.* **9**, 113-120.

Dumas, J. J., Merithew, E., Sudharshan, E., Rajamani, D., Hayes, S., Lawe, D., Corvera, S. and Lambright, D. G. (2001). Multivalent endosome targeting by homodimeric EEA1. *Mol. Cell* **8**, 947-958.

Futter, C. E. and Hopkins, C. R. (1989). Subfractionation of the endocytic pathway: isolation of compartments involved in the processing of internalised epidermal growth factor-receptor complexes. *J. Cell Sci.* **94**, 685-694.

Gorman, R. M. and Poretz, R. D. (1987). Resolution of multiple endosomal compartments associated with the internalization of epidermal growth factor and transferrin. *J. Cell Physiol.* **131**, 158-164.

Hamasaki, M., Araki, N. and Hatae, T. (2004). Association of early endosomal autoantigen 1 with macropinocytosis in EGF-stimulated A431 cells. *Anat. Rec. A Discov. Mol. Cell. Evol. Biol.* **277**, 298-306.

Hanover, J. A., Willingham, M. C. and Pastan, I. (1984). Kinetics of transit of transferrin and epidermal growth factor through clathrin-coated membranes. *Cell* **39**, 283-293.

Hopkins, C. R., Miller, K. and Beardmore, J. M. (1985). Receptor-mediated endocytosis of transferrin and epidermal growth factor receptors: a comparison of constitutive and ligand-induced uptake. *J. Cell Sci.* **3**, 173-186.

Hopkins, C. R., Gibson, A., Shipman, M. and Miller, K. (1990). Movement of internalized ligand-receptor complexes along a continuous endosomal reticulum. *Nature* **346**, 335-339.

Katzmann, D. J., Stefan, C. J., Babst, M. and Emr, S. D. (2003). Vps27 recruits ESCRT machinery to endosomes during MVB sorting. *J. Cell Biol.* **162**, 413-423.

Keating, E., Nohe, A. and Petersen, N. O. (2007). Studies of distribution, location and dynamic properties of EGFR on the cell surface measured by image correlation spectroscopy. *Eur. Biophys. J.* **37**, 469-481.

Lakadamyali, M., Rust, M. J. and Zhuang, X. (2006). Ligands for clathrin-mediated endocytosis are differentially sorted into distinct populations of early endosomes. *Cell* **124**, 997-1009.

Lawe, D. C., Patki, V., Heller-Harrison, R., Lambright, D. and Corvera, S. (2000). The FYVE domain of early endosome antigen 1 is required for both phosphatidylinositol 3-phosphate and Rab5 binding. Critical role of this dual interaction for endosomal localization. *J. Biol. Chem.* **275**, 3699-3705.

Lawe, D. C., Chawla, A., Merithew, E., Dumas, J., Carrington, W., Fogarty, K., Lifshitz, L., Tuft, R., Lambright, D. and Corvera, S. (2002). Sequential roles for phosphatidylinositol 3-phosphate and Rab5 in tethering and fusion of early endosomes via their interaction with EEA1. *J. Biol. Chem.* **277**, 8611-8617.

Maxfield, F. R. and McGraw, T. E. (2004). Endocytic recycling. *Nat. Rev. Mol. Cell. Biol.* **5**, 121-132.

Merithew, E., Stone, C., Eathiraj, S. and Lambright, D. G. (2003). Determinants of Rab5 interaction with the N terminus of early endosome antigen 1. *J. Biol. Chem.* **278**, 8494-8500.

Merrifield, C. J., Perrais, D. and Zenisek, D. (2005). Coupling between clathrin-coated-pit invagination, cortactin recruitment, and membrane scission observed in live cells. *Cell* **121**, 593-606.

Mills, I. G., Jones, A. T. and Clague, M. J. (1998). Involvement of the endosomal autoantigen EEA1 in homotypic fusion of early endosomes. *Curr. Biol.* **8**, 881-884.

Mobius, W., Herzog, V., Sandhoff, K. and Schwarzmann, G. (1999). Intracellular distribution of a biotin-labeled ganglioside, GM1, by immunoelectron microscopy after endocytosis in fibroblasts. *J. Histochem. Cytochem.* **47**, 1005-1014.

Orth, J. D., Krueger, E. W., Weller, S. G. and McNiven, M. A. (2006). A novel endocytic mechanism of epidermal growth factor receptor sequestration and internalization. *Cancer Res.* **66**, 3603-3610.

Patki, V., Virbasius, J., Lane, W. S., Toh, B. H., Shpetner, H. S. and Corvera, S. (1997). Identification of an early endosomal protein regulated by phosphatidylinositol 3-kinase. *Proc. Natl. Acad. Sci. USA* **94**, 7326-7330.

Patki, V., Buxton, J., Chawla, A., Lifshitz, L., Fogarty, K., Carrington, W., Tuft, R. and Corvera, S. (2001). Insulin action on GLUT4 traffic visualized in single 3T3-l1 adipocytes by using ultra-fast microscopy. *Mol. Biol. Cell* **12**, 129-141.

Penengo, L., Mapelli, M., Murachelli, A. G., Confalonieri, S., Magri, L., Musacchio, A., Di Fiore, P. P., Polo, S. and Schneider, T. R. (2006). Crystal structure of the ubiquitin binding domains of rabex-5 reveals two modes of interaction with ubiquitin. *Cell* **124**, 1183-1195.

Pike, L. J., Han, X. and Gross, R. W. (2005). Epidermal growth factor receptors are localized to lipid rafts that contain a balance of inner and outer leaflet lipids: a shotgun lipidomics study. *J. Biol. Chem.* **280**, 26796-26804.

Progida, C., Malerod, L., Stuffers, S., Brech, A., Bucci, C. and Stenmark, H. (2007). RILP is required for the proper morphology and function of late endosomes. *J. Cell Sci.* **120**, 3729-3737.

Puri, C., Tosoni, D., Comai, R., Rabellino, A., Segat, D., Caneva, F., Luzzi, P., Di Fiore, P. P. and Tacchetti, C. (2005). Relationships between EGFR signaling-competent and endocytosis-competent membrane microdomains. *Mol. Biol. Cell* **16**, 2704-2718.

Raiborg, C., Bache, K. G., Mehlum, A., Stang, E. and Stenmark, H. (2001a). Hrs recruits clathrin to early endosomes. *EMBO J.* **20**, 5008-5021.

Raiborg, C., Bremnes, B., Mehlum, A., Gillooly, D. J., D'Arrigo, A., Stang, E. and Stenmark, H. (2001b). FYVE and coiled-coil domains determine the specific localisation of Hrs to early endosomes. *J. Cell Sci.* **114**, 2255-2263.

Schlessinger, J., Schreiber, A. B., Levi, A., Lax, I., Libermann, T. and Yarden, Y. (1983). Regulation of cell proliferation by epidermal growth factor. *CRC Crit. Rev. Biochem.* **14**, 93-111.

Sigismund, S., Woelk, T., Puri, C., Maspero, E., Tacchetti, C., Transidico, P., Di Fiore, P. P. and Polo, S. (2005). Clathrin-independent endocytosis of ubiquitinated cargos. *Proc. Natl. Acad. Sci. USA* **102**, 2760-2765.

Simonsen, A., Lippe, R., Christoforidis, S., Gaullier, J. M., Brech, A., Callaghan, J., Toh, B. H., Murphy, C., Zerial, M. and Stenmark, H. (1998). EEA1 links PI(3)K function to Rab5 regulation of endosome fusion. *Nature* **394**, 494-498.

Sonnichsen, B., De Renzis, S., Nielsen, E., Rietdorf, J. and Zerial, M. (2000). Distinct membrane domains on endosomes in the recycling pathway visualized by multicolor imaging of Rab4, Rab5, and Rab11. *J. Cell Biol.* **149**, 901-914.

Sorkina, T., Huang, F., Beguinot, L. and Sorkin, A. (2002). Effect of tyrosine kinase inhibitors on clathrin-coated pit recruitment and internalization of epidermal growth factor receptor. *J. Biol. Chem*. **277**, 27433-27441.

Stenmark, H., Aasland, R., Toh, B. H. and D'Arrigo, A. (1996). Endosomal localization of the autoantigen EEA1 is mediated by a zinc-binding FYVE finger. *J. Biol. Chem.* **271**, 24048-24054.

Su, X., Kong, C. and Stahl, P. D. (2007). GAPex-5 mediates ubiquitination, trafficking, and degradation of epidermal growth factor receptor. *J. Biol. Chem.* **282**, 21278-21284.

Tosoni, D., Puri, C., Confalonieri, S., Salcini, A. E., De Camilli, P., Tacchetti, C. and Di Fiore, P. P. (2005). TTP specifically regulates the internalization of the transferrin receptor. *Cell* **123**, 875-888.

Trischler, M., Stoorvogel, W. and Ullrich, O. (1999). Biochemical analysis of distinct Rab5- and Rab11-positive endosomes along the transferrin pathway. *J. Cell Sci.* **112**, 4773-4783.

Willingham, M. C., Haigler, H. T., Fitzgerald, D. J., Gallo, M. G., Rutherford, A. V. and Pastan, I. H. (1983). The morphologic pathway of binding and internalization of epidermal growth factor in cultured cells. Studies on A431, KB, and 3T3 cells, using multiple methods of labelling. *Exp. Cell Res.* **146**, 163-175.

Willingham, M. C., Hanover, J. A., Dickson, R. B. and Pastan, I. (1984). Morphologic characterization of the pathway of transferrin endocytosis and recycling in human KB cells. *Proc. Natl. Acad. Sci. USA* **81**, 175-179.

Wilson, J. M., de Hoop, M., Zorzi, N., Toh, B. H., Dotti, C. G. and Parton, R. G. (2000). EEA1, a tethering protein of the early sorting endosome, shows a polarized distribution in hippocampal neurons, epithelial cells, and fibroblasts. *Mol. Biol. Cell* **11**, 2657-2671.

Yamazaki, T., Zaal, K., Hailey, D., Presley, J., Lippincott-Schwartz, J. and Samelson, L. E. (2002). Role of Grb2 in EGF-stimulated EGFR internalization. *J. Cell Sci.* **115**, 1791-1802.

Yarden, Y. (2001). The EGFR family and its ligands in human cancer. signalling mechanisms and therapeutic opportunities. *Eur. J. Cancer* **37 Suppl. 4**, S3-S8.

Yarden, Y. and Schlessinger, J. (1985). The EGF receptor kinase: evidence for allosteric activation and intramolecular self-phosphorylation. *Ciba Found. Symp.* **116**, 23-45.